






# Ladies in armor: A micro-computed tomographic study of skin calcification in European toads (genus *Bufo*)

Milena Cvijanović<sup>1</sup>  | Maja Ajduković<sup>1</sup>  | Jan W. Arntzen<sup>2,3</sup>  |  
Ana Ivanović<sup>3,4</sup>  | Tijana Vučić<sup>2,3,4</sup> 

<sup>1</sup>University of Belgrade, Institute for Biological Research “Siniša Stanković”, National Institute of Republic of Serbia, Belgrade, Serbia

<sup>2</sup>Leiden University, Institute of Biology, Leiden, The Netherlands

<sup>3</sup>Naturalis Biodiversity Center, Leiden, The Netherlands

<sup>4</sup>University of Belgrade, Faculty of Biology, Belgrade, Serbia

## Correspondence

Tijana Vučić, Institute of Biology, Leiden University, Leiden, Sylviusweg, 72, 2333BE The Netherlands.  
Email: [t.vucic@biology.leidenuniv.nl](mailto:t.vucic@biology.leidenuniv.nl)

## Funding information

Naturalis Biodiversity Center; Ministry of Education, Science and Technological Development of the Republic of Serbia, Grant/Award Numbers: 451-03-68/2022-14/200007, 451-03-68/2022-14/200178; Universiteit Leiden

## Abstract

Micro-computed tomography is a powerful tool toward the detailed reconstruction of internal and external morphology, in particular for ossified and other dense tissues. Here, we document and compare the level of calcification in the skin of the head and the parotoids (the external skin glands) in males and females of common and spined toads, *Bufo bufo* and *B. spinosus*. In some anurans, including *Bufo* species, a specific acellular calcified tissue layer within the dermis has been documented (the Eberth-Katschenko, or EK-layer). By a combination of micro-computed tomography and classical histology, we detected additional calcium deposits located in the dermal layer *stratum spongiosum*, positioned above the EK-layer. We showed that the level of calcification and the presence of additional calcium deposits are size and sex related, increasing in the order *B. bufo* males, *B. spinosus* males, *B. bufo* females to *B. spinosus* females. The last of these groups is the least variable. *Bufo spinosus* females have dense calcium deposits in the parotoids and the dorsal and ventral skin. Three-dimensional volume renderings and cross-sectional slices obtained by micro-CT scanning indicate that this approach is a promising technique for further studies on bufonid skin anatomy and geographic variation in skin calcification.

## KEYWORDS

additional calcium deposits, *Bufo spinosus*, *Bufo bufo*, head skin, volume rendering

## 1 | INTRODUCTION

The amphibian skin consists of two layers, the outer epidermis and the inner dermis. The dermis is composed of two layers: the *stratum spongiosum* which contain loose connective tissue with blood vessels and glands and the *stratum compactum* made of collagenous fibers

(Fox, 1986; Duellman and Trueb, 1994). Some anurans possess a calcified layer between the aforementioned two layers (Elkan, 1968; Toledo and Jared, 1993a; Azevedo et al., 2005). This structure is known by various names: the Eberth-Katschenko or EK-layer (Elkan, 1968), ground substance (Elkan, 1976), calcified layer (Toledo and Jared, 1993a, 1993b), mineralized dermal layer

This is an open access article under the terms of the [Creative Commons Attribution-NonCommercial-NoDerivs](https://creativecommons.org/licenses/by-nc-nd/4.0/) License, which permits use and distribution in any medium, provided the original work is properly cited, the use is non-commercial and no modifications or adaptations are made.

© 2023 The Authors. The Anatomical Record published by Wiley Periodicals LLC on behalf of American Association for Anatomy.

(Katchburian et al., 2001) and *lamina calcarea* (Vickaryous and Sire, 2009). The layer may vary in size and thickness depending on the body part as well as between species and individuals (Elkan, 1968; Toledo and Jared, 1993a; Mangione et al., 2011; Quinzio and Fabrezi, 2012; Ponsa et al., 2017). Calcification increases during ontogeny (Elkan, 1968; Quinzio and Fabrezi, 2012; Chammas et al., 2014) and varies between habitats (Toledo and Jared, 1993a; Barrionuevo, 2017; Mari et al., 2022). The EK-layer is more abundant in the dorsal than in ventral skin (Elkan, 1968; Azevedo et al., 2005) and can be continuous or be distributed in patches. The presence of the EK-layer may be associated with terrestriality, especially in anurans from drier regions (Elkan, 1968; Toledo and Jared, 1993a, 1993b). It has been hypothesized that the EK-layer has a role in protection against body water loss (Elkan, 1968; Toledo and Jared, 1993b; Lillywhite, 2006; Mari et al., 2022) and in mineral homeostasis (Moss, 1972; Verhaagh and Greven, 1982; Bentley, 1984).

Micro-computed tomography (micro-CT) is an imaging tool for the production of series of high-resolution two-dimensional trans-axial projections (or “slices”) of an object which are subsequently combined to produce a three-dimensional (3D) image. We here employ micro-CT together with traditional histological techniques to describe the morphology and the level of calcification of the skin of the head in the two European *Bufo* species. The common toad, *B. bufo* (Linnaeus, 1758) and the spined toad, *B. spinosus* Daudin, 1803 are distributed over the western Palaearctic. *Bufo bufo* has a wide range from the northeast of France and further across Europe into the United Kingdom, Scandinavia, Russia, and the Near East. *Bufo spinosus* has a range from the north of Africa, across the Iberian Peninsula into the southwest of France. The most recent common ancestor of the two species is estimated to have lived in the Late Miocene, at approximately 9.2 mya (Recuero et al., 2012). In spite of a long-lasting independent evolutionary history and deep genetic differentiation, the species are morphologically similar. *Bufo bufo* is generally smaller than *B. spinosus*, but the species show a substantial amount of geographical variation (Cvetković et al., 2009; Gingras et al., 2013). In particular, toads from southern populations appear similar with a large body size and a skin with numerous well-developed warts that have keratinous spines (see de Lange, 1973), yet they represent *B. spinosus* in the western, and *B. bufo* in the central and eastern Mediterranean regions. The species form a narrow hybrid zone that runs from the Atlantic coast in Normandy, France to the Mediterranean coast in Liguria, Italy (Arntzen et al., 2018). In most of this area *B. bufo* and *B. spinosus* can be distinguished by morphology, for example by the positioning of the parotoid

glands that run in parallel or are slightly divergent in *B. bufo* and are more widely divergent in *B. spinosus* (Arntzen et al., 2013). The species may also differ in the amount of keratinization in epidermis (Arntzen et al., 2013; Čadenović et al., 2013). Both species show a significant sexual size dimorphism with females being larger than males (Arntzen, 1999; Lüscher et al., 2001; Dursun et al., 2022; Ivanović et al., 2022).

Here, we measured the level of calcification of the toad head skin and the parotoids. We used micro-CT for the detailed reconstruction of dense tissues in the head region. This approach is especially useful to study well ossified bones (Waltenberger et al., 2021), including the *B. bufo* and *B. spinosus* cranial skeleton (Ivanović et al., 2022). Other dense dermal structures such as osteoderms (Broeckhoven et al., 2017; Paluh et al., 2017; Broeckhoven and du Plessis, 2018; Williams et al., 2022) and epidermal enamel structures (Woodruff et al., 2022) can also be explored with high precision while the material is kept intact. To further investigate skin structures that are visible on the micro-CT scans, we used traditional histology.

Because skin anatomy can be sexually dimorphic and depend on body size (VanBuren et al., 2019), we tested for differences between species and sexes in the level of calcification of the head skin, and whether the level of calcification was related to skull size. We expected higher level of skin calcification in *B. spinosus* than in *B. bufo*. As there is a pronounced sexual dimorphism in the skull size of both species *B. bufo* and *B. spinosus* (Arntzen, 1999; Lüscher et al., 2001; Čadenović et al., 2013; Ivanović et al., 2022; Dursun et al., 2022), we expected that sexual dimorphism would be confirmed for the level of calcification as well.

## 2 | MATERIALS AND METHODS

Thirteen *B. bufo* females, 14 *B. bufo* males, nine *B. spinosus* females and nine *B. spinosus* males preserved in ethanol at the Naturalis Biodiversity Center, Leiden, The Netherlands were scanned with a high-resolution micro-CT scanner (Xradia Versa 520, Carl Zeiss X-Ray Microscopy Inc., Pleasanton, CA, USA), with 80 keV source voltage and 86–88 mA intensity. Collection and locality information can be found in Supporting information, Table S1. The 3D visualization of the data (also known as “volume rendering”) was used to examine the level of calcification with Avizo 9.5 software (FEI, Thermo Fisher Scientific). Using the micro-CT scanner, we recorded calcification of the dorsal and ventral head skin, and the parotoids. Levels of calcification were recorded as absent, light, medium and strong for the dorsal skin and parotoids (Figure 1) whereas calcification

**FIGURE 1** Illustration of the character states describing levels of calcification of the dorsal head skin and the parotoid glands that can be found in both sexes and species of European toads (*Bufo bufo* and *B. spinosus*) exemplifying the levels: (a) absent, (b) light, (c) medium and (d) strong.



was recorded as present or absent for the ventral head skin.

The dorsal head skin of two specimens, with the lowest and highest level of skin calcification observed, was studied by traditional histology. The selected specimens were a *B. bufo* male (ZMA.RenA.9291\_m3) and *B. spinosus* female (ZMA.RenA.5345a; Figure 2) (Supporting information, Table S1). Tissue was fixed in 4% neutral buffered formaldehyde (Centrohema, Serbia) for 24 hr (Bancroft and Gamble, 2002). The tissue was then dehydrated with increasing grades of ethanol solution (30–100%), cleared in xylene and embedded in Histowax (Histolab Product AB, Göteborg, Sweden). Serial cross tissue sections (5  $\mu$ m thickness) were taken with a rotary microtome (RM 2125RT Leica, Wetzlar, Germany). For general skin morphology, Mayer's hematoxylin counterstained with eosin (H&E) staining was performed on deparaffinized and rehydrated tissue sections. The results of this procedure include blue nuclei, red cytoplasm and dark-red muscles. For the histological visualization of calcium deposits in tissue sections we used the commercially available Abcam Von Kossa kit (ab150687) (Sheehan and Hrapchak, 1980) following manufacturer's instructions. The results of this procedure include black or dark brown calcium in mass deposits, red nuclei and pink cytoplasm. Additionally,

we used Masson's trichrome staining which may work to distinguish cells from the connective tissue. The results of this staining include dark brown to black stained nuclei, red/reddish cytoplasm and muscle fibers, as well as the blue appearance of collagen.

Digital images of stained sections were made on a LEITZ DM RB light microscope (Leica Mikroskopie & Systems GmbH, Wetzlar, Germany), with a LEICA DFC320 CCD camera (Leica Microsystems Ltd., Heerbrugg, Switzerland) and analyzed with Leica DFC Twain Software (Leica, Germany).

## 2.1 | Statistical analysis

Fisher's exact test for count data was performed to test for statistical significance in character states frequency distribution. As an estimation of head size, we used skull size data obtained from the same individuals (centroid size values—CS; Supporting information, Table S1) from Ivanović et al. (2022). To test if the individuals with different levels of calcification of dorsal skin and parotoids differ in skull size, we performed a nested ANOVA with calcification level, species and sex nested within species as factors and skull size as dependent variable. We did not analyze the ventral skin in this test because

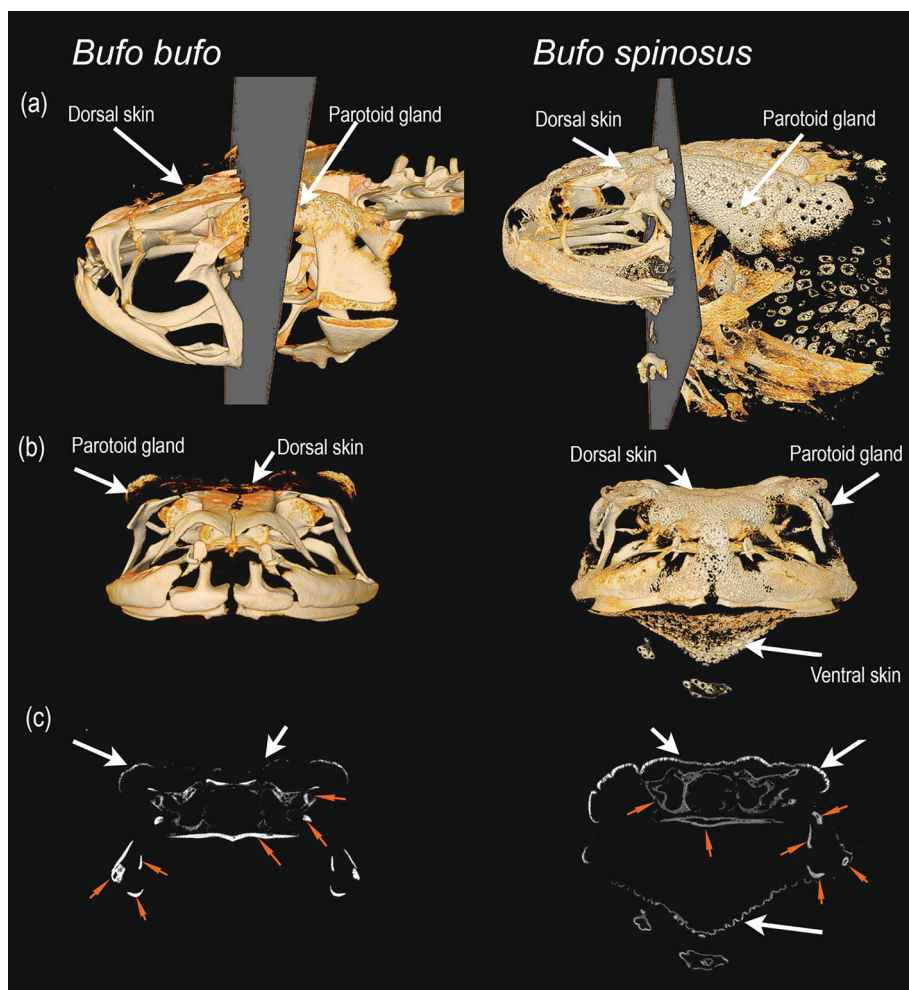


**FIGURE 2** Volume renderings in lateral (a) and frontal (b) view of the head region in a *Bufo bufo* female and a *B. spinosus* female, with arrows pointing to calcification sections of the skin and the parotoids. Specimen collection numbers are ZMA.RenA.9291\_f20 and ZMA.RenA.5345a, respectively. The lower panel (c) shows a cross-section at the position of the parotoids, with the small orange arrows pointing to cross-sections of cranial bones. Gray surfaces in lateral view (a) represent the position of a cross-sectional virtual slice presented in (b) and (c).

calcification was observed in *B. spinosus* females only. Statistical analyses were performed using R version 4.0.2 (R core team, 2020).

### 3 | RESULTS

Using the micro-CT technique we observed substantial variation in the level of calcification of the toad's head skin and parotoids (Table 1, Figures 1 and 2). *Bufo spinosus* females stood out compared to conspecific males and *B. bufo* on account of a strong calcification of the dorsal and ventral skin, as well as the parotoids. A low level of dorsal calcification characterized *B. bufo* males with no detectable calcification of the parotoids as a character state only observed in this group (Table 1).

Using traditional histological techniques we detected and confirmed the presence of the EK-layer as well as additional calcium deposits (ACDs) in the skin of European toads. Sections of the dorsal skin revealed a clearly visible epidermis and a dermis with two layers, namely the *stratum spongiosum* and the *stratum compactum* with the calcified EK-layer in between in both

**TABLE 1** Character state distributions with the number of individuals with the specific state of character observed for the level of calcification in females and males of *Bufo bufo* and *B. spinosus*.

Character	State	<i>B. bufo</i>		<i>B. spinosus</i>	
		Females N = 13	Males N = 14	Females N = 9	Males N = 9
Parotoids	Strong	8	3	9	7
	Medium	4	4	0	2
	Light	1	3	0	0
	Absent	0	4	0	0
Dorsal skin	Strong	0	0	6	0
	Medium	8	1	2	5
	Light	3	6	1	3
	Absent	2	7	0	1
Ventral skin	Present	0	0	6	0
	Absent	13	14	3	9

species (Figure 3). The ACDs were present in the *stratum spongiosum* just above the EK-layer (Figure 3b,c,d). The positive reaction obtained with the Von Kossa technique

**FIGURE 3** Histological overview of cross sections of dorsal skin from *Bufo bufo* male (ZMA.RenA.9291\_m3) and *B. spinosus* female (ZMA.RenA.5345a), with (a) *B. bufo* skin stained with hematoxylin and eosin, (b) *B. spinosus* skin stained with hematoxylin and eosin, (c) *B. spinosus* skin stained with Von Kossa kit and (d) *B. spinosus* skin stained with Masson's trichrome. All micrographs are 10× magnification (bar = 200 μm). ACD, additional calcium deposit; CH, chromatophores; EK, Eberth-Katschenko layer; EP, epidermis; M, muscle; SC, *stratum compactum*; SS, *stratum spongiosum*.

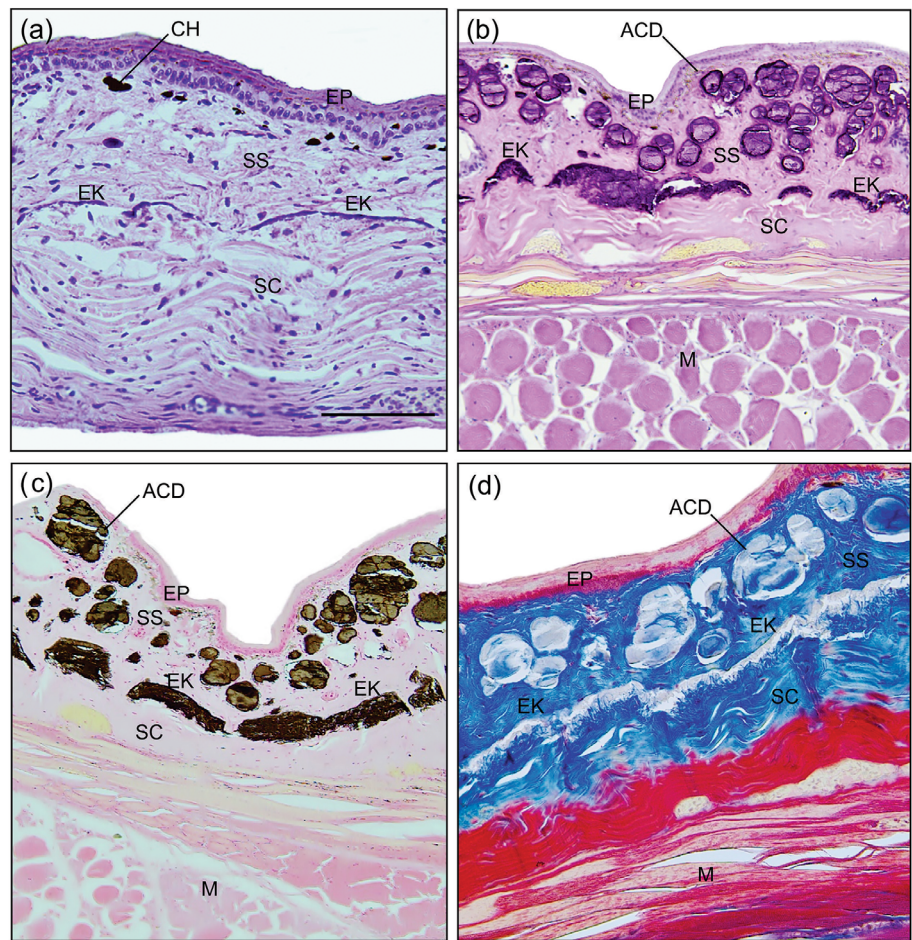


**TABLE 2** Relationship between skull size (CS) as dependent variable and calcification level, species and sex nested within species tested by nested ANOVA.

	Calcification level			Species			Species (sex)		
	Df, error	F	p	Df, error	F	p	Df, error	F	p
Dorsal skin	2, 31	93.73	<0.0001	1, 31	4.28	0.0470	5, 31	4.58	0.0030
Parotoids	3, 33	13.26	<0.0001	1, 33	18.78	<0.0001	4, 33	12.85	<0.0001

confirmed that skin sections contained acellular calcium phosphate deposits in the EK-layer and in the ACDs (Figure 3c). Using the Masson's trichrome staining we confirmed the presence of collagen fibers which were clearly visible in the ACDs (Figure 3d). As judged by their anatomical position, shape and clustering, the ACDs correspond to superficial structures that are well-visible on the micro-CT virtual cross sections and volume renderings.

Species and sexes significantly differed in the level of calcification (Fisher's exact test,  $p < 0.001$ ) and pairwise comparisons showed that groups differed from one another ( $p < 0.05$ ). A nested ANOVA indicated that the level of calcification of the head skin was related to skull

size. The effects of species and sex on the calcification levels were also significant, but less pronounced (Table 2, Figure 4). For the parotoids, the effect of calcification was similar for species and sex (Table 2).

## 4 | DISCUSSION

We used micro-CT as well as traditional histology to study the level of calcification of the head skin in the common (*Bufo bufo*) and the spined toad (*B. spinosus*). We found that the species have the same general skin morphology, including ACDs positioned above the EK-layer, most pronounced so in *B. spinosus* females. The

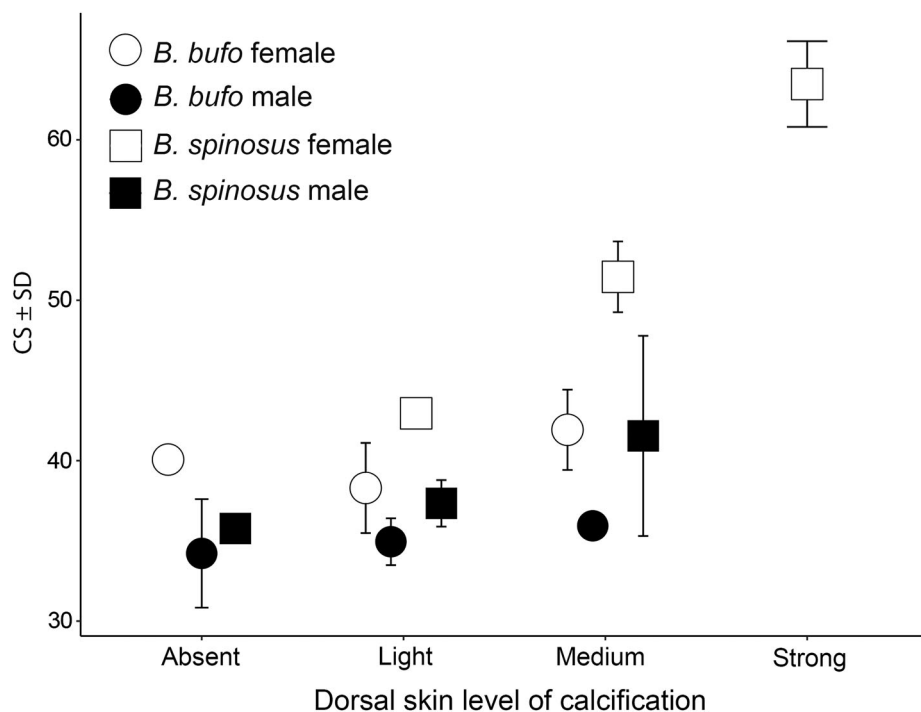


**FIGURE 4** Mean skull size (centroid size—CS) for *Bufo bufo* and *B. spinosus* individuals with different scores of dorsal skin calcification level. Samples sizes and character state distributions are presented in Table 1.

EK-layer and ACDs are separated from the underlying skull bones and should not be confused with co-ossification that was reported for some bufonids (Duellman and Trueb, 1994; Navas et al., 2002; Paluh et al., 2020; Mailho-Fontana et al., 2022). Similar ACDs, in the form of irregular acellular structures dispersed in the *stratum spongiosum*, have also been found in *Rhinella icterica* (syn. *Bufo ictericus*) (Azevedo et al., 2005, 2006) and *Bufotes sitibundus* (syn. *Bufotes variabilis*) (Mutlu et al., 2019) and were described as a part of the EK-layer. Compared with the above mentioned species, the ACDs in *B. spinosus* are well-separated and positioned above the EK-layer (Figure 3b,c,d). It has been claimed that the EK-layer is the remnant of a dermal skeleton in an anuran ancestor for which the arguments are that it has the same position, embryonic origin and mineral components as in osteoderms (Mangione et al., 2011). Yet other authors noted that the calcified skin structures evolved independently in many tetrapod lineages (Vickaryous and Sire, 2009). There is, for example, a marked similarity (homoplasy) in position and structure of osteoderms in the gecko *Geckolepis maculate* (Paluh et al., 2017) and the ACDs newly described in *Bufo* toads.

The ACDs are more abundant in *B. spinosus* than in *B. bufo* and in females than in males. The highest concentrations are found at the level of the warts and the parotoids. Despite substantial variation within species, our results indicate that *B. bufo* and *B. spinosus* differ in the level of calcification of skin and parotoids, with significant effects of size and sex. Body size is affected by a

multitude of ecological and evolutionary factors, including sexual selection, and may be correlated with physiological and fitness traits (Blanckenhorn, 2000). In amphibians, body size and skin permeability have crucial roles in the regulation of water content (Ponssa et al., 2017; VanBuren et al., 2019) and is often related to climatic factors (Toledo and Jared, 1993b; de Brito-Gitirana and Azevedo, 2005; Young et al., 2005). The thickness of the skin could be indicative of its capacity to minimize water loss (Kobelt and Linsenmair, 1986; Lillywhite 2006) which is crucial for anuran survival. In support of this notion is the substantial geographical variation in body size and keratinized integument structures (cheek warts and spines) in *B. bufo* and *B. spinosus* (de Lange, 1973; Lüscher et al., 2001; Cvetković et al., 2009; Čadenović et al., 2013). Also, body size could associate with sexual dimorphism in skin thickness (VanBuren et al., 2019). We found that the level of head skin calcification was positively related to skull size which coincided with a marked, female biased sexual size dimorphism (Arntzen, 1999; Lüscher et al., 2001; Čadenović et al., 2013; Ivanović et al., 2022; Dursun et al., 2022). Yet, the calcification level of the head skin and the parotoids cannot be solely explained by size.

A female biased sexual dimorphism in the level of dermal bones calcification (osteoderms) has been also recorded in lizards (Broeckhoven and du Plessis, 2022). It has been proposed that the higher level of calcification in females serves as a mineral reserve necessary for eggshell

formation (Broeckhoven and du Plessis, 2022). In amphibians, the mineral storage hypothesis cannot be directly related to reproduction. However, other physiological processes and functional roles may underlie the skin calcification dimorphism (Moss, 1972; Verhaagh and Greven, 1982; Bentley, 1984).

If we assume that ACDs have similar functional roles in homeostasis and protection from desiccation as the EK-layer, the calcification of the skin might be related to the habitat (Elkan, 1968; Moss, 1972; Toledo and Jared, 1993a; Brito-Gitirana and Azevedo 2005; Lillywhite 2006; Felseburgh et al. 2009; Mari et al., 2022) whereas Ponssa and coauthors (2017) noted a strong phylogenetic signal of EK-layer thickness. Further research is necessary to determine whether ACDs are common to the genus *Bufo* and to discover how this trait evolved across bufonids.

Although the *B. bufo* and *B. spinosus* specimens investigated herein represent just a part of the species distribution across Eurasia, we demonstrated a significant effect of species, size and sexual dimorphism on the calcification level of skin and parotoids. We envisage that a wider sampling regime across the geographic range of both species and ontogenetic series would help to unravel the complex relationships between the parameters and processes driving the female biased armouring in common toads. Because micro-CT technique allows quantification of the level of calcification without destruction of the material, it would be an appropriate tool for studies of larger series of collection material of whole specimens. In addition, the less dense, soft tissues of the skin which show little contrast in X-rays imagery could be visualized by using iodine-based contrast-enhanced micro-CT imaging (diceCT; Callahan et al., 2021) yielding detailed anatomical insight of the skin ideally across the entire, large clade of bufonids.

## ACKNOWLEDGMENTS

We thank an anonymous reviewer and Alexander Kupfer for constructive comments that helped us to improve the manuscript, as well as Tim D. Smith for his editorial advices and guidance. This study was supported by a Temminck-Fellowship of Naturalis Biodiversity Center to AI, Leiden University and by the Ministry of Education, Science and Technological Development of the Republic of Serbia (grant numbers 451-03-68/2022-14/200007 and 451-03-68/2022-14/200178). We thank Dirk van der Marel for help in optimizing the settings of the Naturalis CT-scanner for the material under study and Esther Don-dorp for collection management.

## DATA AVAILABILITY STATEMENT

All information about the analyzed specimens, including level of calcification and head size (centroid size), is

available as the supporting information. Trans-axial slices (micro-CT obtained virtual slices) of specimen's head region are available at <https://doi.org/10.5061/dryad.gtth76hqv>.

## ORCID

Milena Cvijanović  <https://orcid.org/0000-0001-6258-3983>

Maja Ajduković  <https://orcid.org/0000-0001-9115-6622>

Jan W. Arntzen  <https://orcid.org/0000-0003-3229-5993>

Ana Ivanović  <https://orcid.org/0000-0002-6247-8849>

Tijana Vučić  <https://orcid.org/0000-0002-8850-5251>

## REFERENCES

- Arntzen, J. W. (1999). Sexual selection and male mate choice in the common toad, *Bufo bufo*. *Ethology Ecology and Evolution*, 11, 407–414.
- Arntzen, J. W., McAtear, J., Recuero, E., Ziermann, J. M., Ohler, A., van Alphen, J., & Martínez-Solano, I. (2013). Morphological and genetic differentiation of *Bufo* toads: Two cryptic species in western Europe (Anura, Bufonidae). *Contributions to Zoology*, 82, 147–169.
- Arntzen, J. W., McAtear, J., Butôt, R., & Martínez-Solano, I. (2018). A common toad hybrid zone that runs from the Atlantic to the Mediterranean. *Amphibia Reptilia*, 39, 41–50.
- Azevedo, R. A., Pelli, A. A., Ferreira-Pereira, A., de Jesus Santana, A. S., Felseburgh, F., & de Brito-Gitirana, L. (2005). Structural aspects of the Eberth-Katschenko layer of *Bufo ictericus* integument: Histochemical characterization and biochemical analysis of the cutaneous calcium (Amphibian, Bufonidae). *Micron*, 36, 61–65.
- Azevedo, R. A., de Jesus Santana, A. S., & de Brito-Gitirana, L. (2006). Dermal collagen organization in *Bufo ictericus* and in *Rana catesbeiana* integument (Anuran, Amphibian) under the evaluation of laser confocal microscopy. *Micron*, 37, 223–228.
- Bancroft, J. D., & Gamble, M. (2002). *Theory and practice of histological techniques* (5th ed.). Churchill Livingstone.
- Barrionuevo, J. S. (2017). Skin structure variation in water frogs of the genus *Telmatobius* (Anura: Telmatobiidae). *Salamandra*, 53, 183–192.
- Bentley, P. J. (1984). Calcium metabolism in the Amphibia. *Comparative Biochemistry and Physiology*, 79A, 1–5.
- Blanckenhorn, W. U. (2000). The evolution of body size: What keeps organisms small? *The Quarterly Review of Biology*, 75, 385–407.
- Broeckhoven, C., du Plessis, A., le Roux, S. G., Mouton, P. F. N., & Hui, C. (2017). Beauty is more than skin deep: A non-invasive protocol for in vivo anatomical study using micro-CT. *Methods in Ecology and Evolution*, 8, 358–369.
- Broeckhoven, C., & du Plessis, A. (2018). X-ray microtomography in herpetological research: A review. *Amphibia-Reptilia*, 39, 377–401.
- Broeckhoven, C., & du Plessis, A. (2022). Osteoderms as calcium reservoirs: Insights from the lizard *Ouroborus cataphractus*. *Journal of Anatomy*, 241, 635–640.
- Callahan, S., Crowe-Riddell, J. M., Nagesan, R. S., Gray, J. A., & Davis Rabosky, A. R. (2021). A guide for optimal iodine staining and high-throughput diceCT scanning in snakes. *Ecology and Evolution*, 11, 11587–11603.

- Chammas, S. M., Carneiro, S. M., Ferro, R. S., Antoniazzi, M. M., & Jared, C. (2014). Development of integument and cutaneous glands in larval, juvenile and adult toads (*Rhinella granulosa*): A morphological and morphometric study. *Acta Zoologica*, 96, 460–477.
- Cvetković, D., Tomašević, N., Ficetola, G. F., Crnobrnja-Isailović, J., & Miaud, C. (2009). Bergmann's rule in amphibians: Combining demographic and ecological parameters to explain body size variation among populations in the common toad *Bufo bufo*. *Journal of Zoological Systematics and Evolutionary Research*, 47, 171–180.
- Čadenović, N., Vukov, T., Popović, E., & Ljubisavljević, K. (2013). Morphological differentiation of the common toad *Bufo bufo* (Linnaeus, 1758) in the central part of the Balkan peninsula. *Archives of Biological Sciences*, 65, 685–695.
- de Brito-Gitirana, L., & Azevedo, R. A. (2005). Morphology of *Bufo ictericus* integument (Amphibia, Bufonidae). *Micron*, 36, 532–538.
- de Lange, L. (1973). A contribution to the intraspecific systematics of *Bufo bufo* (Linnaeus, 1758) (Amphibia). *Beaufortia*, 21, 99–106.
- Duellman, W. E., & Trueb, L. (1994). *Biology of amphibians*. Johns Hopkins University Press.
- Dursun, C., Gül, S., & Özdemir, N. (2022). Sexual size and shape dimorphism in Turkish common toads (*Bufo bufo* Linnaeus 1758). *The Anatomical Record*, 305, 1548–1558.
- Elkan, E. (1968). Mucopolysaccharides in the anuran defence against desiccation. *Journal of Zoology*, 155, 19–53.
- Elkan, E. (1976). Ground substance: An anuran defense agent against desiccation. In B. Lofts (Ed.), *Physiology of the Amphibia* (pp. 101–110). Academic Press.
- Felseburgh, F. A., de Almeida, P. G., de Carvalho-E-Silva, S. P., & de Brito-Gitirana, L. (2009). Microscopical methods promote the understanding of the integument biology of *Rhinella ornata*. *Micron*, 40, 198–205.
- Fox, H. (1986). Amphibian skin: dermis. In X. Bereither-Hahn, G. Matoltsy, & K. Sylvia-Richard (Eds.), *Biology of the integument* (pp. 78–110). Springer-Verlag.
- Gingras, B., Boeckle, M., Herbst, C. T., & Fitch, W. T. (2013). Call acoustics reflect size across four anuran clades. *Journal of Zoology*, 289, 143–150.
- Ivanović, A., Cvijanović, M., Vučić, T., & Arntzen, J. W. (2022). Differentiation of skull morphology and cranial kinesis in common toads. *Organisms, Diversity and Evolution*, 2022. <https://doi.org/10.1007/s13127-022-00585-5>
- Katchburian, E., Antoniazzi, M. M., Jared, C., Faria, F. P., Souza Santos, H., & Freymüller, E. (2001). Mineralized dermal layer of the Brazilian tree-frog *Corythomantis greeningi*. *Journal of Morphology*, 248, 56–63.
- Kobelt, F., & Linsenmair, K. E. (1986). Adaptations of the reed frog *Hyperolius viridiflavus* (Amphibia, Anura, Hyperoliidae) to its arid environment. *Oecologia*, 68, 533–541.
- Lillywhite, H. B. (2006). Water relations of tetrapod integument. *The Journal of Experimental Biology*, 209, 202–226.
- Lüscher, B., Grossenbacher, K., & Scholl, A. (2001). Genetic differentiation of the common toad (*Bufo bufo*) in the Swiss Alps. *Amphibia Reptilia*, 22, 141154.
- Mangione, S., Garcia, G., & Cardozo, O. M. (2011). The Eberth-Katschenko layer in three species of ceratophryines anurans (Anura: Ceratophryidae). *Acta Zoologica*, 92, 21–26.
- Mailho-Fontana, P. L., Titon, B., Antoniazzi, M. M., Gomes, F. R., & Jared, C. (2022). Skin and poison glands in toads (*Rhinella*) and their role in defence and water balance. *Acta Zoologica*, 103, 112–128.
- Mari, R. B., Mori, G. M., Vannucchi, F. S., Ribeiro, L. F., Correa, C. N., de Lima, S. K. S., Teixeira, L., Sandretti-Silva, G., Nadaline, J., & Bornschein, M. R. (2022). Relationships of mineralized dermal layer of mountain endemic miniature frogs with climate. *Journal of Zoology*, 318, 34–46.
- Moss, M. L. (1972). The vertebrate dermis and the integumental skeleton. *American Zoologist*, 12, 27–34.
- Mutlu, H. S., Kumaş, M., Akat, E., Yenmiş, M., Çiçek, K., & Ayaz, D. (2019). Histochemical examinations on integument of four anurans: *Bufo bufo*, *Bufo variabilis* (Bufonidae), *Pelophylax bedriagae* (Ranidae), *Hyla savignyi* (Hylidae) from Turkey. *Biharean Biologist*, 13, 28–31.
- Navas, C., Jared, C., & Antoniazzi, M. (2002). Water economy in the casque-headed tree-frog *Corythomantis greeningi* (Hylidae): Role of behaviour, skin, and skull skin co-ossification. *Journal of Zoology*, 257, 525–532.
- Paluh, D. J., Griffing, A., & Bauer, A. M. (2017). Sheddable Armour: Identification of osteoderms in the integument of *Geckolepis maculata* (Gekkota). *African Journal of Herpetology*, 66, 12–24.
- Paluh, D. J., Stanley, E. L., & Blackburn, D. C. (2020). Evolution of hyperossification expands skull diversity in frogs. *Proceedings of the National Academy of Sciences*, 117, 8554–8562.
- Ponssa, M. L., Barrionuevo, J. S., Pucci Alcaide, F., & Pucci, A. A. (2017). Morphometric variations in the skin layers of frogs: An exploration into their relation with ecological parameters in *Leptodactylus* (Anura, Leptodactylidae), with an emphasis on the Eberth-Katschenko layer. *The Anatomical Record*, 300, 1895–1909.
- Quinzio, S., & Fabrezi, M. (2012). Ontogenetic and structural variation of mineralizations and ossifications in the integument within ceratophryid frogs (Anura, Ceratophryidae). *The Anatomical Record*, 295, 2089–2103.
- R Core Team. (2020). *R: A language and environment for statistical computing*. R Foundation for Statistical Computing.
- Recuero, E., Canestrelli, D., Vörös, J., Szabó, K., Poyarkov, N. A., Arntzen, J. W., Crnobrnja-Isailović, J., Kidov, A. A., Cogălniceanu, D., Caputo, F. P., Nascetti, G., & Martínez-Solano, I. (2012). Multilocus species tree analyses resolve the radiation of the widespread *Bufo bufo* species group (Anura, Bufonidae). *Molecular Phylogenetics and Evolution*, 62, 71–86.
- Sheehan, D., & Hrapchak, B. (1980). *Theory and practice of histotechnology* (2nd ed.). Battelle Press.
- Toledo, R. C., & Jared, C. (1993a). The calcified dermal layer in anurans. *Comparative Biochemistry and Physiology Part A: Physiology*, 104, 443–448.
- Toledo, R. C., & Jared, C. (1993b). Cutaneous adaptations to water balance in amphibians. *Comparative Biochemistry and Physiology Part A: Physiology*, 105, 593–608.
- VanBuren, C. S., Norman, D. B., & Fröbisch, N. B. (2019). Examining the relationship between sexual dimorphism in skin anatomy and body size in the white-lipped tree frog, *Litoria infrafrenata* (Anura: Hylidae). *Zoological Journal of the Linnean Society*, 186, 491–500.
- Verhaagh, M., & Greven, H. (1982). Localization of calcium in fibrocytes associated with the "substantia amorpha" in the skin of toad, *Bufo bufo* (L.) (Amphibia, Anura). *Acta Histochemica*, 70, 139–149.



- Vickaryous, M. K., & Sire, J. Y. (2009). The integumentary skeleton of tetrapods: Origin, evolution, and development. *Journal of Anatomy*, 214, 441–464.
- Waltenberger, L., Rebay-Salisbury, K., & Mitteröcker, P. (2021). Three-dimensional surface scanning methods in osteology: A topographical and geometric morphometric comparison. *American Journal of Physical Anthropology*, 174, 846858.
- Williams, C., Kirby, A., Marghoub, A., Kéver, L., Ostashevskaya-Gohstand, S., Bertazzo, S., Moazen, M., Abzhanov, A., Herrel, A., Evans, S. E., & Vickaryous, M. (2022). A review of the osteoderms of lizards (Reptilia: Squamata). *Biological Reviews*, 97, 1–19.
- Woodruff, E. C., Huie, J. M., Summers, A. P., & Cohen, K. E. (2022). Pacific spiny Lumpsucker armor development, damage, and defense in the intertidal. *Journal of Morphology*, 283, 164–173.
- Young, J. E., Christian, K. A., Donnellan, S., Tracy, C. R., & Parry, D. (2005). Comparative analysis of cutaneous evaporative

water loss in frogs demonstrates correlation with ecological habits. *Physiological and Biochemical Zoology*, 78, 847–856.

## SUPPORTING INFORMATION

Additional supporting information can be found online in the Supporting Information section at the end of this article.

**How to cite this article:** Cvijanović, M., Ajduković, M., Arntzen, J. W., Ivanović, A., & Vučić, T. (2023). Ladies in armor: A micro-computed tomographic study of skin calcification in European toads (genus *Bufo*). *The Anatomical Record*, 306(8), 1981–1989. <https://doi.org/10.1002/ar.25170>